Lauric Acid/Pentaerythrityl Monolaurate: A Model Melt Esterification

Part 1.—Kinetics

By Manfred Gordon and Constantine G. Leonis

Department of Chemistry, University of Essex, Wivenhoe Park, Colchester CO4 3SQ

Received 11*th February*, 1974

The study of polyfunctional polycondensates and of the structure of gels is dependent on the availability of link-forming mechanisms which are simple and well understood. Esterification in the melt is a favoured method. Although some melt esterification reactions have been found to be represented by third order kinetics and a mechanism free from measurable complicating effects, the study of esterification of dibasic acids with pentaerythritol (PE) has suggested a substitution effect, whereby each esterified OH accelerates the esterification of the remaining OH in the same PE unit by a factor of about $N = 1.5$. This effect is here confirmed by kinetic analysis of the (non-polymerisable) model system lauric acid/PE and, in more detail, lauric acid/pentaerythrityl monolaurate. Accurate and automated readings of about 300 conversion/time data per run, based on the pressure of evolved steam, were fitted to rival kinetic models, over a range of compositions and temperatures. Computer analysis in terms of standard deviations strongly supports the validity of the substitution effect ($N \sim 1.4$). The results are discussed in the context of previous work on esterification in bulk and in dilute solutions.

In this work the kinetics and statistics of esterification of a monofunctional compound (lauric acid, LA) with polyols is studied in order to throw light on related polyfunctional condensations. For these, Flory [1] and Stockmayer [2] recognised from the start two sources of deviations from the ideal or random intermolecular polycondensation theory, to be expected in principle for all real systems: *substitution effects* (of reacted functionalities on neighbouring unreacted ones) and *cyclisation*, i.e. the competition of intramolecular reactions.

The theory did not furnish error limits for the effects of such deviations on structural parameters (e.g. the gel point) or on physical properties, e.g. the elastic modulus, calculated from the ideal theory. This is serious because even small deviations of either kind can have profound physical effects, e.g. a modest amount of ring formation occurring before gelation is expected to reduce markedly diffusion rates through the gel subsequently formed. Equally seriously, it is difficult to measure the extent of substitution and cyclisation effects; for instance, no direct measurements such as spectroscopic analysis give information on the presence of large rings. The seriousness of this situation is underlined by the observation that the structure of weak gels is of great importance in the life sciences. The preferred method of attack on the problem is a combination of chemical kinetics and statistics, e.g. gel points and various other parameters of molecular distributions. Such a combined study was made [3] on polyesterification in the melt of adipic acid and pentaerythritol (AA/PE) or 1,1,1-tri(hydroxymethyl) ethane(AA/TME). The results showed that, there was a substantial cyclisation effect with a critical conversion or gel point $\beta_c = 0.623$ compared with $3^{-\frac{1}{2}}$ ($= 0.577$) predicted from the ring-free theory for (AA/PE). The full strength of

the effect was partly masked by a moderately strong substitution effect of the positive kind, i.e. an *increase* of rate of esterification of an OH due to each ester group in the same repeat unit. This effect was deduced quantitatively in terms of two parameters N_1 and N_2, which measure the factors by which the esterification rate constant increases in AA or PE, in respect of each previously reacted carboxyl or hydroxyl group carried on the same repeat unit respectively. Results of rate measurements, gel points, dilution with solvent, and statistical calculation of the ring-chain competition effect using known bond lengths and angles, combined to produce the results $N_1 = 0.9 \pm 0.1$ and $N_2 = 1.5 \pm 0.1$. Of these two parameters, only N_2 differs significantly from unity. The reasons for the sensitivity of hydroxyl groups to the prior substitution of neighbouring hydroxyl groups by ester groups were largely a matter for speculation. In terms of the activation energy of esterification, N_2 corresponds to an effect given by

$$N_2 = \exp(-\Delta E^*/2RT) \quad (1)$$

so that $N_2 = 1.5$ gives the very modest $\Delta E^* \approx 3$ kJ mol^{-1} at a temperature of 170°C. The question of the reality and origin of this effect is still topical, even though other esterification systems have since been found, especially decane-1,10-diol/benzene-1,3,5-triacetic acid (DMG/BTA), for which no substitution effect is measurable.[4] Results for the kinetics of esterification and gel points of PE with sebacic and tridecanoic acid fully supported the existence of the substitution effect in PE.[5] The effect in PE should be equally present in esterification in the melt with monofunctional carboxylic acids. Although such systems are in many ways simpler, gelation does not occur, and until recently it was not possible to make reliable measurements of substitution effects.

The present work was undertaken in an effort to establish the substitution effect in esterification of PE with a monocarboxylic acid, using g.p.c. (see Part 2 [6]) to study the distribution statistics of the products [6] (in place of gelation which is not applicable) in conjunction with precise kinetic measurements.

KINETIC SCHEME FOR LA/PE AND LA/PEML

In accordance with previous work on related irreversible self-catalysed esterification reactions, an overall third order reaction scheme is postulated, i.e. first order in hydroxyl groups and second order in carboxyl groups, perturbed by a linear first shell substitution effect (FSSE) among the hydroxyl groups.[3] The basic third order esterification reaction introduces a third order rate constant k^* (taken in units g^2 mol^{-2} min^{-1} for convenience), and the substitution effect introduces a single dimensionless parameter N, where N^i represents the factor multiplying k^* when i previously esterified hydroxyl groups are borne by the reactant PE unit. Accordingly, the following rate equation applies:

$$-\mathrm{d}p_i/\mathrm{d}t = k^*[N^i(4-i)p_i - N^{i-1}(5-i)p_{i-1}]p^2C_L^{\circ 2}. \quad (2)$$

The following notation is employed: p_i denotes the fraction $n_i/\Sigma_i n_i$ of pentaerythritol residues in the system bearing i ester groups; and p the fraction n_L/n_L° of lauric acid residues, which are unsterified. Here n_i is the number of moles of the i-ester of PE and n_L the current number of moles of free LA, while n_L° is the initial number of moles. C_L° is the initial concentration of LA of stoichiometric ratio E in units of moles per gram of system. Similarly $C_{P_j}^\circ$ represents the original concentration of the polyol residues used as starting reactant, each possessing initially j ester groups. The stoichiometric ratio E is defined as:

$$E = (4-j)(C_L^\circ/C_{P_j}^\circ). \quad (3)$$

The rate of change of LA is governed by

$$-\mathrm{d}p/\mathrm{d}t = k^* \sum_i (4-i) N^i p_i p^2 C^\circ_{\mathrm{P}_j} C^\circ_{\mathrm{L}}. \quad (4)$$

The initial conditions for these rate equations for the reaction between PE ($j = 0$) and LA are given as:

$$p_{-1} \equiv 0\,;\; p(0) = 1\,;\; p_i(0) = \delta_{0,i}\,;\; i = 0, 1, 2, 3, 4 \quad (5)$$

(where δ_{ij} is the Kronecker delta), and between pentaerythritol monolaurate (PEML, $j = 1$) and LA:

$$p_0 \equiv 0\,;\; p(0) = 1\,;\; p_i(0) = \delta_{1,i}\,;\; i = 1, 2, 3, 4. \quad (6)$$

For fitting kinetic data, i.e. the evolution in time of the system, computer solutions of eqn (2)-(6) were used. The programme, utilising an improved version written in Algol,[7] is based on Gear's method [8] for solving systems of simultaneous differential equations. For fitting statistical measurements, not involving time directly, explicit solutions are given in Part 2.[6]

EXPERIMENTAL

FACTORS DETERMINING THE CHOICE OF REACTANTS

Because of its high symmetry and H-bonding in the crystal, PE has a high melting point (262°C), and its solubility in lauric acid is insufficient to give a homogeneous equimolar solution in LA below about 195°C. At this temperature the reaction velocity is already so high, as to restrict severely the available temperature range for kinetic studies. A similar situation exists with benzene-1,3,5-triacetic acid/decamethylene glycol condensates BTA/DMG, though it is less severe there (m.p. of BTA 209°C). In that case, the problem was solved [9] by carrying out the esterification reaction in two stages, an initial four minutes at 170°C to achieve dissolution and about 10 % of the esterification, followed by a second stage at some lower temperature for kinetic study. This method was also tried for the system LA/PE but failed, because too much reaction had to be carried out before a homogeneous reaction was obtained, thus invalidating the use of the initial conditions and the proposed rate equations. A second method tried was based on the use of solvents of low vapour pressure for PE and LA, viz. the tribenzhydryl ester of BTA and pentaerythrityl tetralaurate (PETEL), but these were found inadequate solvents for PE. In addition, the presence of PE in reaction products causes trouble in subsequent g.p.c. analysis, because of its insolubility in tetrahydrofuran (THF). The only solution found to these problems was to abandon the first reaction step in the esterification sequence, by using as the starting material PEML [eqn (2), (3), (4), (6)], which has a melting point of 73°C and is miscible with LA above its melting point. The mixture LA/PEML has a convenient temperature range for kinetic study between 150 and 195°C. In addition, a few runs between pentaerythritol and lauric acid were also carried out for comparison at 195°C only.

MATERIALS

Pentaerythritol (PE) was obtained from British Drug Houses Ltd and recrystallized several times from 0.005 equiv. dm^{-3} HCl until big crystals (several mm in size) were formed. The melting point was 261.5°C (lit. 262°C). The percentage of hydroxyl groups was found [10] to be 49.9 % (theoretical 50.0 %).

Lauric acid (LA) was Koch–Light Laboratories Ltd *puriss* grade. It was recrystallized several times from alcohol (m.p. found 45°C, lit. 43-46°C).

Pentaerythrityl monolaurate (PEML) was not available commercially and was prepared and purified in the way described below.

PE powder containing a small amount of LA (to depress the melting point) was placed in the lower part of a glass reactor with a glass-lined magnetic stirrer, while LA was placed in the upper part above a break-seal. The molar ratio of PE : LA was approximately 9 : 1.

Both parts of the apparatus were evacuated to 10^{-4} Torr (to avoid oxidation) and sealed under high vacuum. The apparatus was immersed in a silicone oil bath thermostated at 260°C equipped with a rotating magnetic plate. PE slowly decomposes at 260°C, but this did not materially affect the yield of monoester, as most of the LA is esterified in *ca.* 30 min. The break-seal was broken with the stirrer and the LA started to drip into the PE melt. A large excess of PE was always present and the formation of the monoester was favoured. After about 30 min no further bubbles were formed and the system was quenched.

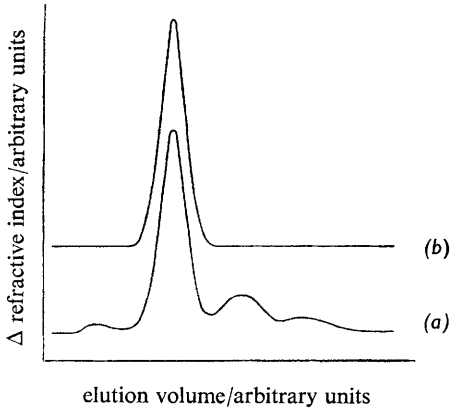

FIG. 1.—Gel permeation chromatograms in THF: (*a*) reaction mixture, (*b*) purified PEML.

The unreacted PE was separated by filtration using THF in which PE is insoluble. The remaining compounds in the mixture except the PEML were LA and higher esters, as shown by the g.p.c. chromatograph in fig. 1(*a*). The monoester was separated from the other compounds by petroleum ether b.p. 60-80°C extraction. After four to five purifications, glass-clear needles were produced, which gave a single-peak and an adequately smooth chromatogram [fig. 1(*b*)]. The melting point was found to be 69°C, though the melt remained turbid to a temperature above 73°C (lit. m.p. = 75°C). The yield of the synthesis was only about 40 %.

PREPARATION OF REACTION MIXTURES

Each reactant was well dried and accurately weighed. The components of the mixture were quantitatively transferred to an agate mortar and were finely ground and thoroughly mixed with the pestle. To assure good mixing the whole mixture was heated gently on a hotplate to 55°C and the resultant paste was again well mixed and ground after cooling. The composition of these mixtures were checked quantitatively by means of g.p.c. Pellets containing *ca.* 100 mg of mixture were made and stored in a silica gel desiccator.

Three mixtures of different stoichiometries, i.e. $E = 1$, $E = \frac{1}{2}$, $E = 2$ were used [eqn (3)]. For the system LA/PE only $E = 1$ was used.

DENSITY DETERMINATIONS OF THE MELTS

The densities of the reactants were measured in a simple dilatometer consisting of a bulb and a precision capillary tube. The volumes of the dilatometers (*ca.* 0.5 cm^3 for the PEML, *ca.* 2.5 cm^3 for the others) were determined with mercury. The samples were put into the dilatometer by means of a syringe taking care to keep everything at a temperature higher than the melting point of the injected compound.

The best straight line between the data pairs of temperature and density furnished the densities of the compounds as a function of temperature. The density coefficients of expansion of the materials used are recorded in table 1.

TABLE 1.—DENSITIES OF THE MELTS

compound	density at 170°C ρ/g cm^{-3}	coefficient of thermal expansion $10^4(d\rho/dT)$/g cm^{-3} K^{-1}	
LA	0.779	−7.2	±0.2
PETEL	0.832	−7.3	±0.2
PEML	0.909	−7.3	±2.0
PE	1.145*	−7.5	±0.5

* extrapolated from ref. (5).

APPARATUS FOR THE KINETICS OF THE ESTERIFICATION

Esterification was followed by the pressure of the steam [3] evolved as a function of time at fixed temperatures in the range 150-195°C. The cylindrical aluminium block thermostat is described first, followed by the pressure transducer measuring system and its calibrations.

The Al block (fig. 2), an improved version of that used earlier,[3-5] was encased in asbestos wool and composition insulation, and had central viewing ports A for observation of the glass apparatus, heating wires B, C and a contact thermometer for crude thermostating to ±0.05°C. The axial tunnel containing the glass apparatus was placed horizontally, which gave much better spatial temperature uniformity than the earlier vertical arrangement.[3] The fine temperature control system (±0.002°C), superposed upon the crude control just mentioned, employed a movable silicone oil cup (fig. 3) which could be positioned around the bottom of the reaction vessel containing the pellet (causing it to melt). The oil cup temperature was controlled at 1 or 2°C above that of the Al block.

The oil-cup (fig. 3) together with the rigidly attached button magnet is rotated around the stationary frame holding the insulated heating wire (Thermocoax) and thermistor (Stantel type GT 15) regulating head, causing the oil to be stirred. A magnetic follower inside the reaction vessel at the same time stirs the reaction melt.

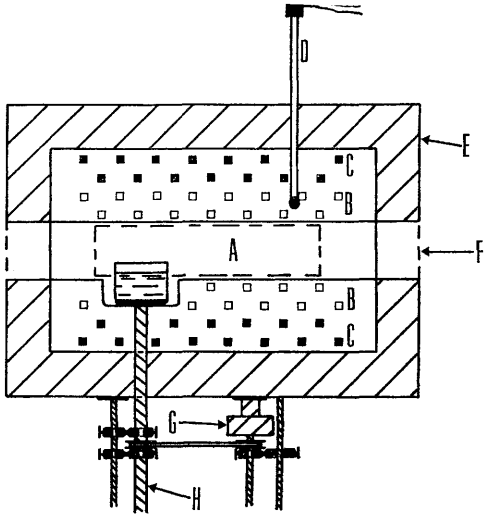

FIG. 2.—Sectioned front view of thermostat aluminium block. A, tunnel for glass reactor (not shown, see fig. 4), and viewing window (dotted line); B, C, heating wires; D, contact thermometer; E, asbestos composition insulator; F, entry port for glass reactor and final position of transducer; G, motor for driving oil cup (fig. 3); H, supporting rod for oil cup.

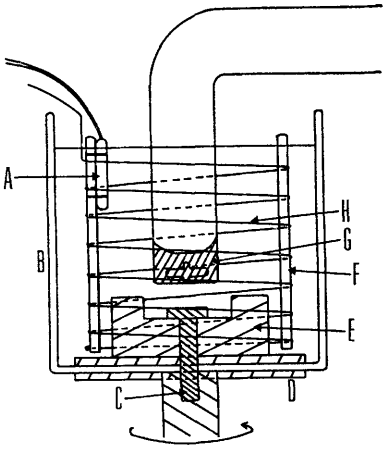

FIG. 3.—Oil cup for fine temperature control. A, thermistor head; B, glass cup; C, threaded screw securing glass cup to supporting rod with leak-proof silicone rubber insulation; D, Teflon washer; E, magnet fixed solidly to oil cup; F, frame for heating wire; G, reaction melt; H, insulated heating wire (Thermocoax).

It is essential to delay the start of the reaction until thermal equilibrium is attained around the transducer measuring head (on the right of fig. 4), because of the sensitivity of this device to temperature changes. To implement such delay, the apparatus is designed so as to allow temperature control of the reaction mass independently of that of the transducer, which is deliberately placed as far as 25 cm away. A sharp start to the reaction can be achieved

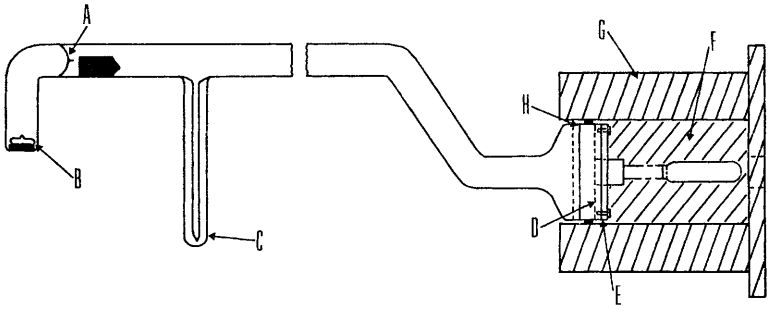

FIG. 4.—Reaction vessel and transducer assembly (schematic): A, break-seal; B, pellet of reactants and magnetic stirrer; C, capillary side-arm; D, transducer diaphragm; E, glass-metal seal; F, air-space; G, asbestos composition plug; H, glass-metal seal to reaction vessel. The reactor volume is *ca.* 30 cm^3.

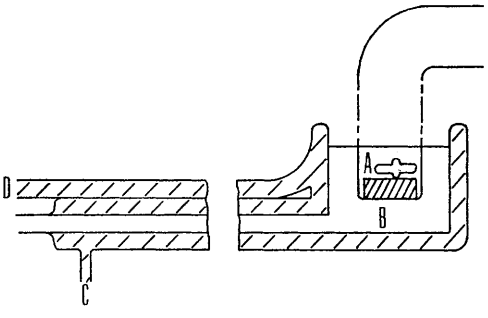

FIG. 5.—Pellet cooling device. A, pellet and magnetic stirrer; B, static oil; C, inlet for circulating water; D, outlet.

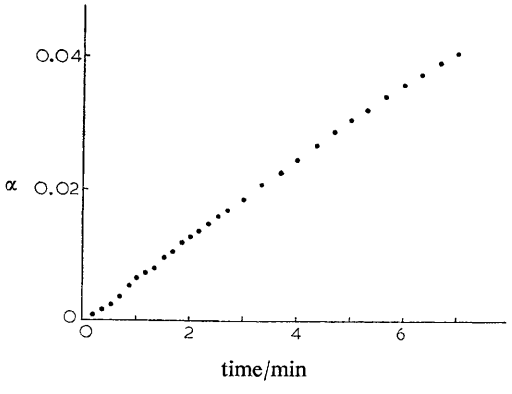

FIG. 6.—Initial part of rate plot for typical reaction. Conversion α is plotted against time using data from transfer unit (see text).

when desired, by exchanging the cooling cup (fig. 5) for the oil heating cup which takes about 10 s. The pellet is seen to melt almost at once. Judged by the smoothness of the rate curve (fig. 6), the melt reaches substantially the temperature of the oil cup within one or two minutes.

THE PRESSURE TRANSDUCER MEASURING SYSTEM AND ITS CALIBRATIONS

The kinetics were followed in terms of the pressure of steam in the sealed reaction vessel, using type 4-316 transducer from Consolidated Electrodynamics, Bell and Howell, U.S.A. The reference side of the transducer contained a small pressure of argon. The glass reaction vessel and the argon reference cell were connected to the transducer by glass-metal seals. When connected to its ripple-free power supply (Solartron strain gauge power supply type A S 974.2), the transducer gave an output linear in the diaphragm pressure. This output was amplified by a Fylde type FE-164-BD/C amplifier, temperature controlled to ± 1°C. The amplified signal was passed to a Solartron multi-channel data transfer unit, connected to a Solartron auto-ranging digital volt-meter. A Facit high-speed papertape punch recorded times and voltages automatically. Calibration measurements of transducer voltage V in mV against *air pressure* (P in Torr) using a Hg manometer at the two extreme temperatures used for the kinetic runs fit a linear relation:

$$P = 727.1(\pm 0.3) - 4.889\ V \quad (\theta = 150°C) \tag{7a}$$

$$P = 652.4(\pm 0.3) - 4.681\ V \quad (\theta = 195°C). \tag{7b}$$

The calibration constant (slope) was reproducible to within 0.15 % for several calibrations. It was thought desirable to check the calibration against *steam pressure*, in case there was any interference by sorption or interaction of steam with the measuring device. A thin-walled pear-shaped glass microampoule was weighed, filled almost completely with water (*ca.* 20 mg), sealed and re-weighed. It was placed in the reaction vessel and kept cool by the cooling cup (fig. 5) until the Al block had reached thermal equilibrium at 160°C. When the cooling cup was exchanged for the oil cup, the thermal expansion of the water cracked the micro-ampoule. There was some time delay due to super-heating of residual water in the microampoule, but after about 12 min a steady pressure (*ca.* 1.5 atm) was reached. This pressure accounted for the weighed water to within 2 %, which was considered satisfactory.

DESCRIPTION OF KINETIC RUN USING STEAM PRESSURE MEASUREMENTS

A pellet (*ca.* 90 mg) of reactants, weighed to ± 0.1 mg, and a glass covered magnetic follower were introduced (fig. 4) into the reaction vessel, which was then sealed under vacuum, taking precautions to keep the pellet cool to avoid premature reaction. The reaction vessel was glassblown onto the transducer assembly, leading via the capillary side arm C to a vacuum line and pumped down to 10^{-4} Torr. After the pressure had fallen to the required level (which took several hours), the transducer and the adjacent part of the reaction vessel were baked out at 200°C with an electric heating tape to remove volatile species. Then the seal A was broken by a steel weight and an external magnet exposing the pellet to vacuum. Pelletising the monomers prevents any fines being sucked down the vacuum line. The breakable seal acts as a precaution against loss of monomer (especially lauric acid) during the initial prolonged exposure to high vacuum. The bottom of the reaction vessel was immersed in hot water until the pellet began to melt and immediately recooled. This freed any trapped vapours or air in the pellet, which otherwise later interfered with determining the base line and the starting point by causing a sudden jump in pressure when the pellet melted.

When the pressure had again fallen to its previous level the whole line was flushed several times with dry argon and again evacuated to remove any residual oxygen. The reaction vessel was then sealed at the point C (fig. 4) under a pressure of 20-30 Torr of dry argon (to suppress distillation of lauric acid at the early stages of the reaction, when the part of the reaction vessel just above the treating cup is still below the block temperature.) The transducer reaction vessel assembly was then introduced into the Al block. After thermal equilibrium was reached in the transducer head (constant voltage reading), the data transfer

unit was set to punch out values of time and voltage [at intervals Δ(conversion) $\equiv \Delta\alpha \sim$ 0.002-0.003], the cooling cup was removed and the oil cup was raised to submerge the tip of the reaction vessel and the rotation of the oil cup started.

VAPOUR PRESSURE OF THE REACTANTS

Despite the relatively high pressure of pure liquid LA ($\sim$11 Torr at 170°C), the liquid mixtures of LA with PE and PEML had no measurable vapour pressure. This is seen by extrapolation to zero time of the rate curves, i.e. there was no measurable jump in pressure immediately after heating the melt to 195°C. The implication is that the vapour pressure of LA above the mixture falls far short of that predicted from Raoult's law. It is not surprising that such deviations from ideal solution behaviour in LA/PE and LA/PEML should occur (e.g. due to differences in H-bonding when compared to pure liquid LA).

MEASUREMENT OF THE VOLUME OF THE REACTION VESSEL

After the completion of a kinetic run, the volume of the vessel was determined by connecting it to a gas burette, and evacuating both. The pressure in the reaction vessel was increased in increments, by opening alternately taps connecting the burette to the atmosphere and to the reaction vessel. A plot of $\log(P_a - P_i)$ against i is found to be linear in accordance with Boyle's law, where P_a is atmospheric pressure, and P_i the pressure after the ith increment. The volume of the vessel is calculated from the slope, and found to be reproducible to 0.1 % by least-squares analysis.

RESULTS

DATA PROCESSING OF PRESSURE MEASUREMENT OF EXTENT OF REACTION

Altogether 23 kinetic runs are reported here as set out in table 2, out of a total of 36 runs. Those discarded were suspected of errors due to accidents from various sources during the prolonged time of execution of a run. Each run comprised about 300 voltage (pressure) measurements collected by the data transfer unit and fig. 7 shows the smoothness of the reaction as attested by a typical trace of pressure against time. The pressure of water vapour for each point was calculated from the calibration (see Experimental section). Each pressure reading was then converted to the corrected [11] specific volume of steam $V_{sp,corr}$ at that temperature and this together with the reaction vessel volume V_R, was used to calculate the mass of water $m(t)$ given off and hence the conversion:

$$\alpha(t) = \frac{V_R/V_{sp,corr}(t)}{m(\infty)} = \frac{m(t)}{m(\infty)}, \tag{8}$$

where $m(\infty)$ denotes the mass of the products at full conversion. The mean of each set of runs at fixed E and T was used to construct a mean kinetic curve. Chebychev polynomials of the order 14 or 15 were then fitted to a number ($\sim$100) of data pairs from each of these mean kinetic curves and the polynomials were used to regenerate the curve for all further analyses as described below. A typical plot (fig. 8) of the difference between the averaged experimental extents of reaction and those reproduced by the polynomial shows these differences to be negligible, since $\sigma_{poly} \approx 0.0005$ (table 4, column 5) and the absence of any systematic trend.

FITTING OF RATE LAWS TO THE DATA

Two separate one-parameter theories will be compared. The first formally adjusts the apparent reaction order n as a parameter, the second adjusts the linear first-shell substitution effect (FSSE), parameter N [cf. eqn (2), (4)].

TABLE 2.—OPTIMISED FIT TO APPARENT REACTION ORDER SCHEME

E [eqn(3)]	temp./°C	apparent reaction order, n	correlation coefficient $\times 10^{-1}$	k/g^{n-1} mol^{1-n} min^{-1}	stand. dev. of k over points/ g^{n-1} mol^{1-n} min^{-1}	$10^3 \times$ init. slope/ min^{-1}
1	150	2.70	9.9965	97	2.82	4.90
1	150	2.70	9.9963	96	1.69	5.10
1	160	2.80	9.9987	252	5.75	7.92
1	160	2.80	9.9988	250	8.37	6.51
1	160	2.70	9.9886	134	5.42	8.35
1	160	2.70	9.9974	135	6.33	5.75
1	160	2.80	9.9986	268	7.82	7.43
1	160	2.70	9.9996	138	2.84	7.11
1	160	2.80	9.9996	256	10.14	6.71
1	170	2.80	9.9998	518	20.41	12.76
1	170	2.80	9.9998	486	16.23	14.25
1	170	2.80	9.9998	477	14.90	13.28
1	180	2.80	9.9998	567	21.14	15.81
1	180	2.80	9.9998	577	21.45	14.94
1	180	2.80	9.9998	581	22.32	14.94
1	195	2.70	9.9998	567	9.65	30.03
1	195	2.80	9.9998	1111	34.7	28.75
1*	195	2.70	9.9995	434	16.43	29.2
1*	195	2.70	9.9995	442	17.62	31.24
2	160	2.50	9.8775	40.8	4.02	11.90
		3.00	9.9715	937	99.26	
2	160	2.50	9.8883	39.9	4.05	10.07
		3.00	9.9756	927	99.9	
1/2	160	2.50	9.9820	32.5	2.18	4.47
		3.00	9.9965	870	49.7	
1/2	160	2.50	9.9832	33.4	2.09	4.06
		3.00	9.9958	900	57.69	

* starred entries refer to LA/PE non-starred to LA/PEML.

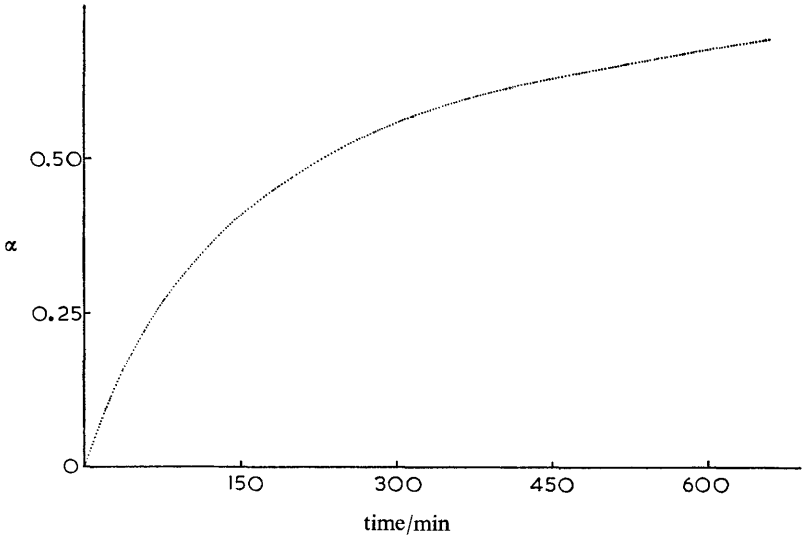

FIG. 7.—Typical kinetic run: conversion α [eqn (8)] against time (at final α = 0.7 the pressure is 202 Torr).

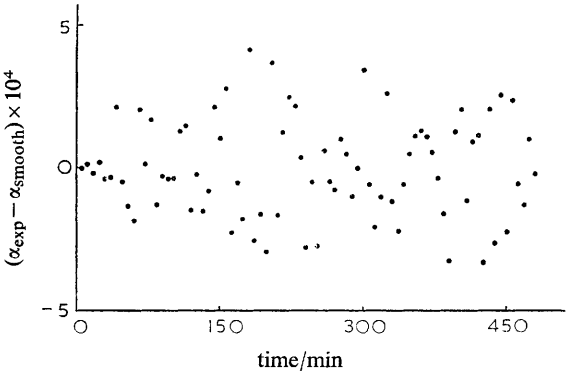

FIG. 8.—A typical plot showing the difference between an original kinetic run and its smoothed reproduction. LA/PEML = 1, θ = 170°C.

APPARENT REACTION ORDER

The absence of a substitution effect ($N = 1$) reduces eqn (2) to the special case of

$$\mathrm{d[COOH]/d}t = k[\mathrm{COOH}]^2[\mathrm{OH}] \tag{9}$$

where the concentrations are expressed as equivalents of the functional groups per unit mass:

$$[\mathrm{COOH}] = (4-j)p^2C_{\mathrm{L}}^{\circ} \tag{10}$$

($j = 0$ for PE/LA and $j = 1$ for PEML/LA), while the hydroxyl concentration is given by

$$[\mathrm{OH}] = \{1-E(1-p)\}C_{\mathrm{P}_j}^{\circ} = \{1/(4-j)\}\sum_{i=j}^{3}(4-i)p_iC_{\mathrm{P}j}^{\circ}. \tag{11}$$

The special case ($n = 3$) can formally be generalised:

$$\mathrm{d[COOH]/d}t = k[\mathrm{COOH}]^{n-1}[\mathrm{OH}]. \tag{12}$$

Let the initial concentration of carboxyl and hydroxyl groups be C_0 and C_0/E (in equivalents of functional groups per unit volume) respectively, and C the carboxyl concentration at time t. If

$$A = (1-E)/E, \tag{13}$$

then

$$-\mathrm{d}C/\mathrm{d}t = k(AC_0+C)C^{n-1}. \tag{14}$$

Approximating, by neglect of change in volume during the course of the reaction [cf. eqn (18)] solutions of eqn (14) in terms of the conversion α_1 of the carboxyl groups (see fig. 9):

$$\alpha_1 = (C_0-C)/C_0 \tag{15}$$

were used by treating the apparent reaction order n as a parameter in the range $2 \leqslant n \leqslant 3$. The best least-squares fit was computed for each run, as was the product moment correlation coefficient r, defined as

$$r = (1/L)\sum_{1}^{L}\left(\frac{x_i-\bar{x}}{\sigma_x}\right)\left(\frac{y_i-\bar{y}}{\sigma_y}\right), \tag{16}$$

where L is the number of data pairs used, and σ_x is the standard deviation of x values about the mean.

The best fit was verified by noting the value of r, which maximises the correlation (table 2). The least squares fit equation was next utilised to calculate the overall rate constant for the n values used [eqn (14)].

Table 2 shows that the best fit is always for reaction orders between 2.7 and 2.8. For the reaction systems with initial stoichiometric ratio other than 1, the fittings for reaction order 2.50 and 3.00 are given instead of the best fit. Even for those cases the best fit lies between 2.7 and 2.8 as is obvious from fig. 9, where plots for different reaction orders are presented. The fit of the fractional-order scheme is not impressive The apparent rate constant is seen systematically to vary by several percent during the course of a run even for the best n-value as is demonstrated by the typical fig. 10. The percentage error in reaction time is equal to that in the apparent rate constant. The error induced in α is, on average, substantially larger than when fitting the FSSE scheme, discussed in the next section.

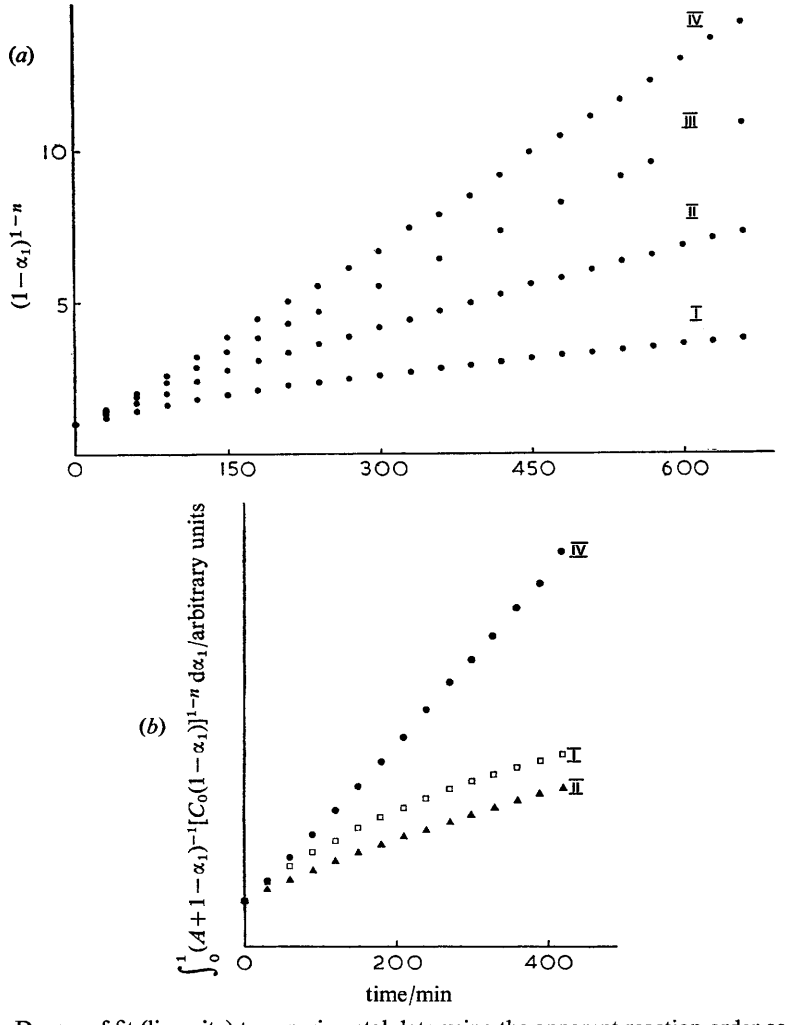

FIG. 9.—Degree of fit (linearity) to experimental data using the apparent reaction order as parameter (*a*) LA/PEML = 1, $\theta = 160°C$; (*b*) LA/PEML = $\frac{1}{2}$, $\theta = 160°C$. I, $n = 2.0$; II, $n = 2.5$; III, $n = 2.8$; IV $n = 3.0$.

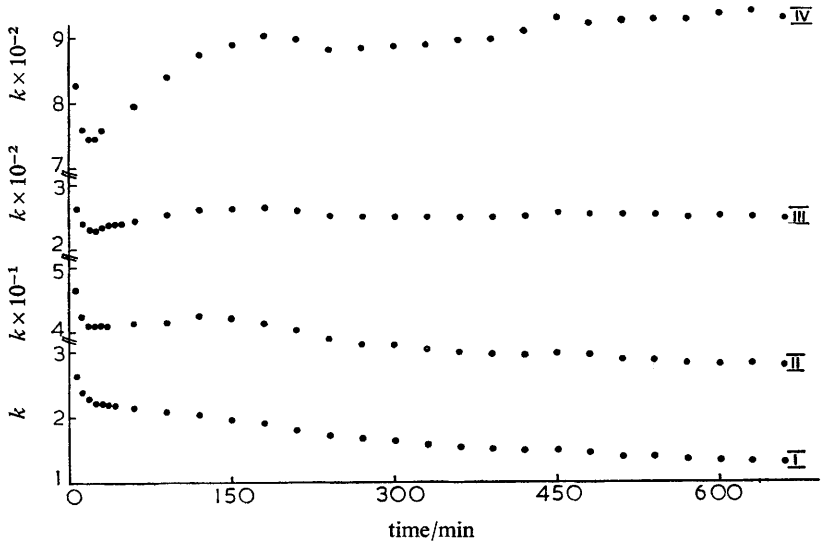

FIG. 10.—Typical plot demonstrating the variation of rate constant with time: I, $n = 2.0$; II, $n = 2.5$; III, $n = 2.8$; IV, $n = 3.0$.

LINEAR FIRST SHELL SUBSTITUTION EFFECT

If the reaction order n is not to be treated as adjustable, a value has to be fixed for it. The true order in the absence of all disturbing effects is thought to be three as shown in solution studies for different esterification systems.[12] Flory confirmed this for bulk esterifications.[13] Gordon and Scantlebury [3] attributed the downward deviation they observed in esterification of PE and TME with adipic acid to cyclisation and substitution effects. Cyclisation is, of course, impossible with monofunctional acids like LA. Estimates of the two parameters k and N are, therefore, calculated using $n = 3$.

The α_{th} values calculated by computer from eqn (2)-(6) at different times were then compared with the corresponding α_{exp} values. Each α_{exp} point was taken from the Chebychev polynomial smoothed mean kinetic curve of the runs for the same reaction conditions.

The standard deviation σ_{fit} is then calculated for various trial values of N and of k^*_{fit} using L ($\sim$50-60) data pairs,

$$\sigma_{fit} = \left(\sum_{1}^{L}(\alpha_{exp}-\alpha_{th})^2/L\right)^{\frac{1}{2}}. \quad (17)$$

Table 3 shows the results of these calculations. The best fit was equated with the minimum of σ_{fit} for given reaction conditions. The quality of the fittings will be discussed from two points of view. First it is seen in table 4 that for the eight rate curves, each of which is the mean of several such curves (23 in all), the standard deviation of the mean measured conversion α from theory was in the range $7 \times 10^{-5} < \sigma_{fit} < 4.7 \times 10^{-3}$. This is an excellent fit of experiment to theory, not significantly affected by the convenient Chebychev polynomial smoothing procedure, since the experimental data are reproduced by the polynomials to a standard deviation of 0.0005.

The second mode of comparison shows more clearly that the fitting of the measurements within experimental error to the particular 1-parameter theory of the linear first-shell substitution effect is highly significant (i.e. in comparison with possible alternative one-parameter fittings).

TABLE 3.—PARAMETERS FROM OPTIMISED FIT TO LINEAR FSSE

stoichiometric E [eqn (3)]	temp./°C	polyol	k^*_{fit}/ g^2 mol^{-2} min^{-1}	N	i	$k_{init.}$/ g^2 mol^{-2} min^{-1}	$k^*_{fit}N^i$/ g^2 mol^{-2} min^{-1}	k^*_{fit}/ g^2 mol^{-2} min^{-1}	N'
1	150	PEML	331	1.45	1	470	480	326	1.38
1	160	PEML	491	1.40	1	668	687	477	1.34
1	170	PEML	915	1.43	1	1261	1309	911	1.35
1	180	PEML	1010	1.47	1	1430	1485	1001	1.39
1	195	PEML	1977	1.45	1	2760	2867	1958	1.37
2	160	PEML	501	1.39	1	705	696	490	1.36
1/2	160	PEML	483	1.53	1	727	739	488	1.44
1	195	PE	1754	1.42	0	1660	1754	1612	1.35

In fig. 11 which is typical for runs at all eight reaction conditions, the difference $\Delta\alpha$ between the conversions taken (*a*) from the Chebychev-smoothed mean reaction curve for the runs at 160°C and of stoichiometric ratio 1 : 1, and (*b*) from four calculated rate curves, are plotted. These curves refer to the substitution effect parameter N adjusted to 1.0 (absence of effect), 1.2, 1.4 and 1.5. It is apparent that an excellent fit is obtained using $N = 1.4$, when the maximum deviation over the range included (up to $\alpha = 0.75$ of total conversion) is $\Delta\alpha = 0.002$. The transformation of plot I to a plot resembling III is clearly a severe test for any one-parameter theory, and the success lends support to the assumption of a substitution effect.

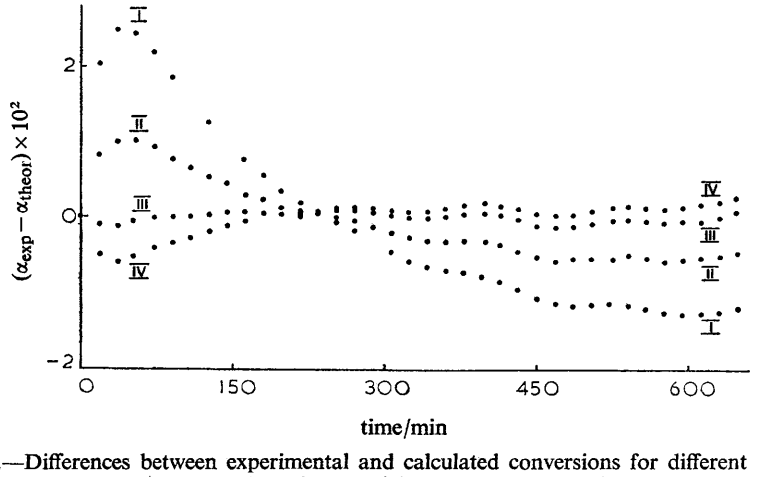

FIG. 11.—Differences between experimental and calculated conversions for different values of the FSSE parameter are plotted against time. LA/PEML = 1, θ = 160°C, I, $N = 1.00$, $k^* = 887$; II, $N = 1.20$, $k^* = 640$; III, $N = 1.40$, $k^* = 491$; IV, $N = 1.50$, $k^* = 436$. k^* in g^2 mol^{-2} min^{-1}.

COMPARISON WITH INITIAL SLOPES

It is inherent in the substitution effect theory, and the fittings just discussed, that the initial part of each rate curve is asymptotic to the case $N = 1$ for PE (i.e. the first few ester links cannot be affected by the substitution effect). This means that in the case of LA/PE the rate constant k^*_{fit} from the optimal fitting (table 3) should equal the

third order constant $k_{\text{init.}}$ calculated from the initial slope. In the case LA/PEML, k^*_{fit} should equal N times $k_{\text{init.}}$, because the starting material PEML is subject to a rate increase by a factor N when fitting eqn (2), (4), (6), since it already contains one ester group. Table 3 shows good agreement between $k_{\text{init.}}$ and k^*_{fit}.

EFFECT OF VOLUME CONTRACTION ON MASS LAW KINETICS

The effect of volume change on the chemical kinetics is now examined. The appropriate theory has been derived [14] on the basis of the equation:

$$\frac{\mathrm{d}(N_i/V)}{\mathrm{d}t} = \frac{1}{V}\frac{\mathrm{d}N_i}{\mathrm{d}t} - \frac{N_i}{V^2}\frac{\mathrm{d}V}{\mathrm{d}t} \tag{18}$$

where N_i is the number of molecules of compound i in volume V, which has an initial value ($t = 0$) V_0.

Applying the above equation to the present situation of esterification in the melt, the law of mass action for a reaction of overall order 3 reads:

$$\frac{\mathrm{d}n_{\mathrm{L}}}{\mathrm{d}t} - \frac{n_{\mathrm{L}}}{V}\frac{\mathrm{d}V}{\mathrm{d}t} = k^*_{\mathrm{v}} n_{\mathrm{L}}^2 n_1 / V^2 \tag{19}$$

where n_1 is the number of moles of PEML in the mixture, and k^*_{v} is the rate constant expressed in dm^6 equiv.$^{-2}$ min^{-1}. If the volume contraction parameter is represented by μ ($\mu > 0$) then at any time t:

$$V = V_0[1-\mu(1-n_{\mathrm{L}}/n^\circ_{\mathrm{L}})] = V_0(1-\mu\alpha). \tag{20}$$

The value of μ is calculated from the stoichiometry and the densities assuming ideal volume mixing

$$\mu = \frac{3V_{\mathrm{m,LA}} + V_{\mathrm{m,PEML}} - V_{\mathrm{m,PETEL}}}{3EV_{\mathrm{m,LA}} + V_{\mathrm{m,PEML}}} \tag{21}$$

where $V_{\mathrm{m},i}$ is the molar volume of compound i at temperature T. By substituting eqn (20) into eqn (19), we obtain

$$\frac{\mathrm{d}n_{\mathrm{L}}}{\mathrm{d}t} = k^*_{\mathrm{v}} n_{\mathrm{L}}^2 n_1 / V_0^2 (1-\mu)(1-\mu\alpha) \tag{22}$$

or in more familiar terms

$$\mathrm{d}p/\mathrm{d}t = k^* p^2[3Np_1 + 2N^2 p_2 + N^3 p_3] C^\circ_{\mathrm{L}} C^\circ_{\mathrm{P_i}} / (1-\mu)[1-\mu(1-p)]. \tag{23}$$

Eqn (23) shows that the correction factor for k^* due to volume change is $(1-\mu)[1-\mu(1-p)]$. In earlier work [3] a correction was made to the kinetic data of this kind to allow for the effect of volume contraction during reaction. The effect was found to be fairly small in its effect on N and moreover the formula then used overestimated the effect by a factor of 2. The shrinkage at full conversion for AA/PE was estimated to be 35 %. In the present case the shrinkage for full conversion was calculated from the measured densities to be 7.2 % for a stoichiometric mixture of LA/PEML at 170°C and 9.4 % for LA/PE at 195°C. To estimate the effect of the volume contraction on the parameter N the factor $1/(1-\mu)[1-\mu(1-p)]$ was incorporated into the differential eqn (2)-(6) and the optimal values for k'_{fit} and N' were obtained (table 3). The average of optimum values for N is thus lowered from 1.42 to 1.37.

ASSESSMENT OF ACCURACY

Table 4 summarises the accuracies of measurements and fittings in terms of the four standard deviations introduced. The reproducibility of steam pressure at fixed

times in different runs is measured by σ_{rep}, the averaged standard deviation from the mean curve for each set of experimental curves at fixed E and T. The error in α introduced by smoothing with Chebychev polynomials is given by σ_{poly}, which was found to lie in the range $1 \times 10^{-4} \leqslant \sigma_{poly} \leqslant 7 \times 10^{-4}$. This may be taken to represent also the standard deviation in some measurement of $\Delta\alpha \approx 0.01$, say, in a given run (cf. fig. 11). The accuracy of absolute measurements of α is around 0.005. The accuracy of fitting the rate curves (averaged over a set of replicate runs) to the kinetic scheme is measured by σ_{fit}. Incorporation of the small volume correction described in the previous section changes σ_{fit} to σ'_{fit}, without conclusive improvement.

TABLE 4.—STANDARD DEVIATIONS FOR THE VARIOUS FITTINGS

stoichiometry E [eqn (3)]	temp./°C	polyol	$\sigma_{repr} \times 10^3$	$\sigma_{poly} \times 10^3$	$\sigma_{fit} \times 10^3$	$\sigma'_{fit} \times 10^3$
1	150	PEML	1.462	0.49	1.95	1.87
1	160	PEML	4.357	0.68	0.664	1.79
1	170	PEML	4.909	0.10	0.081	0.227
1	180	PEML	1.458	0.17	0.100	0.218
1	195	PEML	1.108	0.13	0.094	0.200
2	160	PEML	1.778	0.61	4.68	4.59
1/2	160	PEML	1.652	0.10	0.073	0.092
1	195	PE	1.301	0.14	0.180	0.392

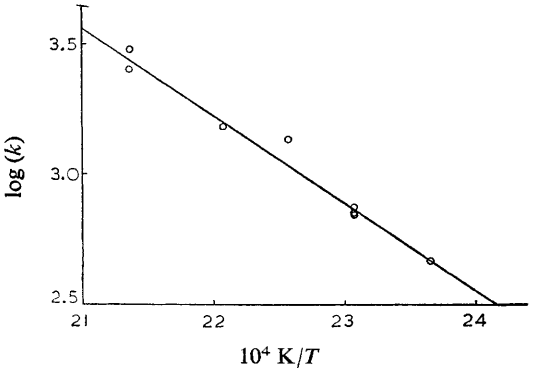

FIG. 12.—Arrhenius plot for all sets of reaction conditions.

TABLE 5.—ACTIVATION ENERGIES FOR ESTERIFICATION REACTIONS

system and source	temperature (range)/ °C	activation energy/ kJ mol^{-1}
bulk {LA/PEML, LA/PE} this work	150-195	64.8±2.9
bulk DMG/BTA [9]	80-90	55.2
palmitic acid/cyclohexanol,[18] dilute solution	100-154	64.4
palmitic acid/ethyl alcohol,[18] dilute solution	75-154	63.2

THE ACTIVATION ENERGY

Figure 12 presents an Arrhenius plot of the 23 runs on LA/PEML and LA/PE, in which the values of the rate constant were optimised over each set of reaction conditions. The activation energy is found from the slope to be 64.8±2.9 kJ mol^{-1}. This is compared in table 5 with results relating to other mono- and poly-functional esterifications, which are seen to be very similar. Rate constants have been measured

in the past for a number of polyfunctional esterifications in the melt, and some typical ones are included in table 6. Their magnitudes do not differ greatly, supporting the conclusion that the general esterification mechanism is the same.

TABLE 6.—COMPARISON OF ESTERIFICATION RATE CONSTANTS

system and source	temperature/°C	$10^{-2}\times$ rate constant/ $g^2\ mol^{-2}\ min^{-1}$
LA/PEML (this work)	175	9.50
adipic acid/PE [3, 5]	175	4.5_4
sebacic acid/PE [5]	175	4.8_3
tridecanoic acid/PE	180	7.2_7
DMG/BTA [4]	170	5.5

DISCUSSION

The kinetics of self-catalysed esterification reactions of monocarboxylic acids have been extensively studied in solution, using monofunctional alcohols.[15] Several studies have also been published on the kinetics of esterification of polyfunctional acids with polyfunctional alcohols in bulk,[16] or in concentrated solutions,[17] and in the present work as a bridging exercise, a monofunctional acid was esterified with polyfunctional alcohols. A comparison of all these studies shows a remarkable degree of uniformity of the reaction kinetics. The reaction order with respect to COOH is generally found to be two; when (OH) is not buffered by excess, as in dilute alcoholic solutions [18] of carboxylic acid, the order with respect to OH is generally found to be close to unity. Although the early work of Flory [13] led to the postulate of an overall third order reaction scheme for the non-catalysed esterification, in more recent work [19] it was claimed that the reaction rate is directly proportional to the hydrogen ion concentration and assigned a 2.5 order to polyesterifications with weak polyfunctional acids, but this is clearly not borne out by the present much more exact and detailed measurements. The activation energy (see final section of the Results) is generally close to 63 kJ mol^{-1} (table 5). It seems reasonable to assume that the mechanism is essentially identical throughout these reactions.

As shown especially accurately in the present work, the deviations in bulk esterification from overall third order kinetics are so small, that they would normally not be noticed. In this work, the optimal fitting always gave apparent reaction orders between 2.7 and 2.8 (cf. fig. 10), but strong evidence has been presented (fig. 11) that the deviations from third order kinetics are linked specifically to the degree of substitution of the alcohol moiety of the reacting complex. More exactly still they can be covered by a single linear first-shell substitution effect parameter N, there being quite sufficient information content in the measurements to lend conviction to the fitting in fig. 11.

Implicitly, however, such data fittings, and the underlying rate eqn (2)-(6), assume the absence of various disturbing effects, which need justification. The most important such effects are due to changes in medium and (on the basis of the collision theory of chemical kinetics) [18] in the size of reaction partners during the course of reaction. In the work of Fairclough and Hinshelwood [18] with dilute solutions of monofunctional carboxylic acids in monofunctional alcohols, effects of medium and of size are discernible, *not* in the course of any one reaction, but in passing from one reaction system to another. When studying polyfunctional systems in bulk, both effects might, therefore, be expected even in the course of a single reaction, since then both the size of the reagents and the medium change appreciably during the course of the reaction.

Unfortunately one cannot hope to study tree-like (ring-free) gels, or therefore, make significant deductions from model systems, without involving polyfunctional materials in bulk. To illustrate the magnitude of the effects found in dilute solution, the pseudo-second order rate constant increases by over 30 % when changing from butyric to palmitic acid in ethyl alcohol [18] (an effect due to reagent size), and by 100 % when passing from cyclohexanol to ethyl alcohol as solvents for butyric or palmitic acids (an effect of the medium). These effects are clearly comparable in magnitude to our finding a change of ~35 % in rate constant when passing from PEML to penta erythritol dilaurate (PEDL). We shall nevertheless contend (cf. Part 2) [6] that the empirical evidence strongly indicates the absence of size effects in melt esterifications. Indeed we also deduce that a medium effect is absent in the course of a single reaction run in the melt, but here a single fortuitous cancellation is quite possible. All that is required is that the replacement of one OH and one COOH by one ester group happens to leave the " solvent " effectively unchanged in quality as regards its functioning as medium for subsequent esterification during the course of a run.

[1] P. J. Flory, *J. Amer. Chem. Soc.*, 1941, **63,** 3083.
[2] W. H. Stockmayer, *Advancing Fronts in Chemistry* (Reinhold, New York, 1945), vol. 1.
[3] M. Gordon and G. R. Scantlebury, *J. Chem. Soc. B*, 1967, 1.
[4] J. A. Love, *Ph.D. Thesis* (University of Strathclyde, 1968).
[5] T. G. Parker, *Ph.D. Thesis* (University of Strathclyde, 1969).
[6] M. Gordon and C. G. Leonis, *J.C.S. Faraday I*, 1975, **71,** 178.
[7] J. Oliver, Computing Centre, University of Essex, personal communication.
[8] (*a*) C. W. Gear, *Comm. A.C.M.*, 1971, **14,** 185; (*b*) C. W. Gear, *Comm. A.C.M.*, 1971, **14,** 176.
[9] C. A. L. Peniche-Covas, *Ph.D. Thesis* (University of Essex, 1973).
[10] C. L. Ogg, W. L. Porter and C. O. Willits, *Ind. Eng. Chem. Anal.*, 1945, **17,** 394.
[11] *National Engineering Laboratory Steam Tables* (H.M.S.O., Edinburgh, 1964).
[12] A. C. Rolfe and C. N. Hinshelwood, *Trans. Faraday Soc.*, 1934, **30,** 937.
[13] (*a*) P. J. Flory, *J. Amer. Chem. Soc.*, 1937, **59,** 466; (*b*) P. J. Flory, *Principles of Polymer Chemistry* (Cornell U.P., Ithaca, 1953).
[14] (*a*) P. D. Barlett and J. Altschul, *J. Amer. Chem. Soc.*, 1945, **67,** 816; (*b*) B. Delmon, A. Giraud and P. Leprince, *Compt. rend.*, 1957, **244,** 1920; (*c*) J. Hutchinson, R. S. Lehrle, J. C. Robb and J. R. Suggate, *J.C.S. Faraday I*, 1973, **69,** 426.
[15] (*a*) C. N. Hinshelwood and A. R. Legard, *J. Chem. Soc.*, 1935, 587; (*b*) H. Goldschmi d., *Ber.*, 1896, **29,** 2208; (*c*) A. T. Williamson and C. N. Hinshelwood, *Trans. Faraday Soc.*, 19t34, **30,** 1145.
[16] (*a*) P. J. Flory, *J. Amer. Chem. Soc.*, 1939, **61,** 3334; (*b*) R. H. Kienle and A. G. Hovey, *J. Amer. Chem Soc*, 1929, **51,** 509; (*c*) R. H. Kienle, P. A. van der Meulen and F. E. Petke *J. Amer. Chem. Soc.*, 1939, **61,** 2258, 2268; (*d*) R. H Kienle and F. E. Petke, *J. Amer. Chem. Soc.*, 1940, **62,** 1053; (*e*) R. H. Kienle and F. E. Petke, *J. Amer Chem. Soc.*, 1941, **63,** 481.
[17] G. R. Scantlebury, *Ph.D. Thesis* (University of London, 1964).
[18] R. A. Fairclough and C. N. Hinshelwood, *J. Chem. Soc.*, 1939, 593.
[19] (*a*) I. Vansco-Szmercsanyi and E. Makay-Bödi, *J. Polymer Sci. C*, 1968, **16,** 3709; (*b*) A. C. Tang and K. S. Yao, *J. Polymer Sci.*, 1959, **35,** 219.